Chemical Geology 673 (2025) 122525

Contents lists available at ScienceDirect

Chemical Geology

journal homepage: www.elsevier.com/locate/chemgeo

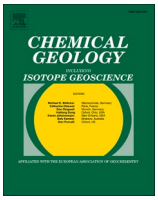

Single quartz $\delta^{18}O$: A new frontier in detrital provenance analysis (Bengal Fan, IODP Expedition 354)

Mara Limonta [a,b,*], Christian France-Lanord [a], Albert Galy [a], Andrey Gurenko [a], Nordine Bouden [a], Eduardo Garzanti [b]

[a] Centre de Recherches Pétrographiques et Géochimiques (CRPG), CNRS – Université de Lorraine, Vandœuvre-lès-Nancy, France
[b] Laboratory of Provenance Studies, Department of Earth and Environmental Sciences, University of Milano-Bicocca, Milano, Italy

ARTICLE INFO

Editor: S. Aulbach

Keywords:
Quartz
Oxygen isotopes
Ion Probe LG-SIMS
Provenance analysis
Single-grain techniques
Himalayan orogen
Bengal fan

ABSTRACT

Quartz is the most abundant mineral in sediments and sedimentary rocks but efforts to reliably identify its provenance have been only partially fruitful so far. Even advanced methods such as cathodo-luminescence, Raman spectroscopy, synchrotron X-ray absorption spectroscopy, and laser ablation spectrometry have led to limited success. This article demonstrates how the $\delta^{18}O$ of detrital quartz provides useful additional insight. The oxygen-isotope signature primarily depends on source rocks and their formation conditions, being highly different for different crustal sources and highest for carbonate rocks.

This study illustrates a new protocol to analyze $\delta^{18}O$ signatures of single quartz grains and shows how provenance from magmatic, metamorphic, or sedimentary domains can be discriminated. In each sand sample from rivers draining exclusively a single Himalayan tectonic domain (e.g., Trans-Himalaya, Greater Himalaya, Lesser Himalaya, and Tethys Himalaya), ~200 quartz grains were analyzed by ion microprobe LG-SIMS (Large Geometry Secondary Ion Mass Spectrometry) to characterize their oxygen-isotope variability. In each turbidite sample collected from the Bengal Fan during IODP Expedition 354, ~150 quartz grains were analyzed next to quantify the relative contribution of each Himalayan domain. This allowed us to complement data obtained with other bulk-sediment to single-mineral approaches, thus enhancing provenance resolution and highlight the erosional evolution of the Himalayan-Tibetan orogen through time.

1. Introduction

Quartz is the most abundant mineral in sandstone, because it is contained and shed in abundance from most types of magmatic, metamorphic, and sedimentary rocks, and because it can resist multiple cycles of erosion through geological time (Blatt, 1967a, 1967b; Basu, 1985; Garzanti et al., 2019a). The original source of quartz grains can be inferred by physical or chemical characteristics, including lattice deformation, presence of impurities, trace-element composition and isotopic composition (Clayton et al., 1972; Götze et al., 2001; Götze et al., 2021). Many attempts have been made to infer the provenance of quartz grains using these properties but with only limited success so far.

The aim of this article is to present a new approach based on the distribution of the oxygen isotope signature of single quartz grains from siliciclastic sediments, and to underscore its potential to decipher their provenance. The $\delta^{18}O$ of quartz serves as a valuable provenance tracer (Sridhar et al., 1975; Clayton et al., 1978; Aléon et al., 2002), the fractionation of oxygen isotopes being controlled by formation conditions (Chacko et al., 2001). The $\delta^{18}O_{V\text{-}SMOW}$ of quartz varies widely in host rocks crystallized at different temperatures, from as low as 6 ‰ for magmatic quartz (Taylor Jr and Epstein, 1962; Taylor, 1968) to as high as 40 ‰ for sedimentary quartz (Syers et al., 1969; Clayton et al., 1972; Knauth and Epstein, 1976). The $\delta^{18}O$ of magmatic quartz is primarily dependent on crustal contamination and can reach 14 ‰ in peraluminous granites (Taylor Jr and Sheppard, 1986). In metamorphic rocks, $\delta^{18}O$ increases from 10 ‰ to 20 ‰ with decreasing metamorphic temperature (Taylor Jr and Coleman, 1968). Very low-temperature surface processes such as weathering and diagenesis are unable to effectively alter the $\delta^{18}O$ of quartz, thus preserving valuable information on the original source (protosource; Sridhar et al., 1975; Clayton et al.,

* Corresponding author at: Centre de Recherches Pétrographiques et Géochimiques (CRPG), CNRS – Université de Lorraine, Vandœuvre-lès-Nancy, France.
E-mail addresses: mara.limonta@univ-lorraine.fr, mara.limonta1986@gmail.com (M. Limonta), christian.france-lanord@univ-lorraine.fr (C. France-Lanord), albert.galy@univ-lorraine.fr (A. Galy), andrey.gurenko@univ-lorraine.fr (A. Gurenko), nordine.bouden@univ-lorraine.fr (N. Bouden), eduardo.garzanti@unimib.it (E. Garzanti).

https://doi.org/10.1016/j.chemgeo.2024.122525
Received 8 September 2024; Received in revised form 26 November 2024; Accepted 27 November 2024
Available online 3 December 2024

1978).

Our approach is based on oxygen-isotope analysis of single quartz grains using secondary ion mass spectrometry (SIMS), primarily aimed at source-to-sink investigations. The single-grain approach is much more powerful than the bulk-sediment or bulk-quartz approach (Vennemann et al., 1992; Vennemann et al., 1996; Aléon et al., 2002) because in most cases quartz grains are not all derived from a single source but from a wide range of sedimentary, metamorphic, and magmatic sources.

The $\delta^{18}O$ composition of ~3900 quartz grains ranging from 5 μm to 500 μm was determined using a CRPG-Nancy CAMECA IMS 1270-E7 ion microprobe. The instrument ensures high spatial resolution (down to a few μm) and sensitivity high enough to be applied for much smaller individual grain samples than those to be analyzed using the conventional laser-probe BrF_5 method (Sharp, 1990).

Quartz grains were separated from sediments of 10 modern river sediments draining each a single major geological Himalayan domain (e.g., Debon et al., 1986, Trans-Himalaya, Greater Himalaya, Lesser Himalaya, and Tethys Himalaya) to characterize the signature of each domain, and to check whether endmembers are sufficiently distinct to allow for clear provenance discrimination. This approach was tested on 5 modern sediments of the Siang, Brahmaputra, Narayani and Ganga rivers and on 7 samples of Bengal Fan turbidite collected during IODP Expedition 354 and ranging in age from Miocene to Pleistocene. The results prove the usefulness of the technique as an independent tool to detect provenance trends and reconstruct the erosional evolution of the Himalayan orogen through time (18 Ma to <0.3 Ma). It also sets the limits of the approach in the Himalayan context.

2. The challenge of quartz provenance

Quartz is the most abundant mineral in the Earth's crust, where it is found as a common constituent of magmatic, metamorphic, and sedimentary rocks formed in a wide range of geological environments. In sandstones, quartz occurs as monocrystalline or less frequently polycrystalline grains in percentages that may exceed 90 % (Blatt, 1967a; Basu, 1985; Garzanti, 2019a). Because of its mechanical and chemical durability, quartz grains may survive weathering and diagenetic processes and are thus commonly recycled, which poses a major challenge whatever technique is used (Blatt, 1967b; Suttner et al., 1981; Dott, 2003; Garzanti, 2017).

The quartz lattice may exhibit a range of physical and chemical features, including dislocations, point defects, planar defects, microinclusions of minerals or fluids incorporated during crystallization under diverse thermodynamic conditions or by secondary processes, such as weathering, irradiation, diagenesis, or metamorphism (Götze, 2012). These characteristics can be revealed by advanced analytical methods, such as cathodo-luminescence and thermoluminescence (Götze et al., 2001), electron paramagnetic resonance spectroscopy (Weil, 1984; Götze et al., 2004), synchrotron X-ray absorption-spectroscopy (Kelly et al., 2008), together with spatially resolved trace-element analysis (Ackerson et al., 2015) such as laser-ablation inductively-coupled-plasma mass-spectrometry and secondary-ion mass-spectrometry (SIMS, Heck et al., 2011). Such sophisticated analyses complement microscopic techniques (polarising microscopy, scanning electron microscopy, transmission electron microscopy, micro-Raman spectroscopy) and trace-element analysis, providing detailed information about the type of impurities and their abundance.

2.1. Limitation of petrographic methods

The origin of quartz grains is traditionally determined in thin section under the petrographic microscope, together with optical properties such as undulatory extinction, polycrystallinity, and number of crystal units (Bokman, 1952a, 1952b; Folk, 1980; Basu, 1985). Polycrystalline quartz tends to be less abundant and more coarsely crystalline in plutonic than metamorphic rocks and for geometrical reasons its abundance increases with grain size in sand. Undulosity and crystallinity features can be modified after deposition during very-low-grade metamorphic deformation at temperatures as low as 200–300 °C (Carter et al., 1964; Blatt et al., 1980; Garzanti and Brignoli, 1989). Despite decades of investigations, distinguishing between first-cycle and polycyclic quartz grains has remained as unsolved problem.

2.2. Limitations of cathodo-luminescence analysis

Cathodo-luminescence is a powerful tool to reveal the presence of impurities in the crystal lattice, internal features, growth zones, and variations in the crystalline structure of quartz grains (Zinkernagel, 1978; Sprunt et al., 1978; Matter and Ramseyer, 1985; Owen and Carozzi, 1986; Walderhaug and Rykkje, 2000; Augustsson and Reker, 2012; Augustsson et al., 2019). A relationship between luminescence colours and crystallization temperature has been established, showing that quartz from high-temperature volcanic or plutonic and contact-metamorphic rocks appears as blue-violet or red-violet, whereas brown shades are typical of lower-temperature metamorphic quartz, and authigenic quartz is typically non-luminescent (Ramseyer et al., 1988; Ramseyer and Mullis, 1990; Götze et al., 2001). During the last decades, however, such colour scheme has been questioned because common overlaps or changes during electron bombardment have been observed (Neuser et al., 1989; Boggs Jr et al., 2002). Different gradations of luminescence colours may be related to other factors, including the degree of lattice order, subsequent mechanical deformation, Al concentration, Ti/Fe ratio, and occurrence of trace elements such as Mn. Even a refined approach combining cathodo-luminescence and scanning-electron-microscopy introduced to reduce ambiguities (Seyedolali et al., 1997; Bernet and Bassett, 2005; Bernet et al., 2007; Hooker and Laubach, 2007) proved to be insufficient to robustly distinguishing between vein and metamorphic quartz or among different granitoid sources (Müller and Knies, 2013).

2.3. Limitations of the other approaches (trace elements and OH defects)

Trace elements are useful to distinguish primary crystallization environments (Götze and Plötze, 1997; Jacamon and Larsen, 2009; Breiter et al., 2013) and different source rocks of detrital quartz. In particular, Ti and Al have been used to assess the relative contribution of different granitoid types to river sediments (Ackerson et al., 2015). However, diverse combinations of trace elements may result from the temperature, pressure, and chemical environments under which plutonic and volcanic rocks crystallize, which prevents us from establishing criteria of general validity also because overlaps exist between volcanic and metamorphic conditions.

The type and abundance of defects found in the quartz lattice are also dependent on pressure, temperature, and chemical system, and can thus provide information on petrogenetic conditions useful in provenance analysis (e.g., Stalder, 2014; Jaeger et al., 2019; Stalder et al., 2024).

Experimental data and observations of natural samples suggest that the most common OH defect (AlOH) is negatively correlated with crystallization pressure (Stalder and Konzett, 2012; Baron et al., 2015; Frigo et al., 2016), and that OH defects tend to decrease with age (Stalder et al., 2017). The assignment of a single quartz grain to a specific source rock type based on infrared absorption spectroscopy (IFR) alone, however, is far from univocal, because even similar rocks from different localities may exhibit strong differences in OH-defect content (Stalder and Neuser, 2013).

Both quartz lattice defects and trace elements control the variation of the quartz optically stimulated luminescence (OSL) sensitivity (Aitken, 1985, 1998; Götze and Möckel, 2012; Williams et al., 2018), which is proposed as provenance indicator. The OSL variability is firstly attributed to source rocks (Chang and Zhou, 2019; Capaldi et al., 2022; Timar-Gabor et al., 2023; Zhang et al., 2023) but also to sedimentary processes acting on the grain after it has been weathered from the original source

rock (e.g. Pietsch et al., 2008; Jeong and Choi, 2012; Sawakuchi et al., 2011). However, the mechanisms of quartz OSL sensitization remain unclear and the relationships between each luminescence emission of quartz and the corresponding responsible defects are generally rather tentative, and the assignments given by different studies are often in contrast with one another (Williams et al., 2022).

2.4. Oxygen isotopes

The limited success of traditional methods has led to propose the use of oxygen isotopes as a provenance tracer (Blatt, 1987). Isotope fractionation depends on quartz crystallization or recrystallization temperature, which allows us to distinguish between high-temperature igneous and low-temperature metamorphic origin of a quartz grain (Clayton and Epstein, 1958, 1961). Most silicate rocks show positive $\delta^{18}O$ values ranging from +5 ‰ to +15 ‰. Mafic rocks and chondritic meteorites plot in a narrow range of lower $\delta^{18}O$ (from +5.5 to +5.9 ‰; Taylor, 1968) than other rocks, the highest values (i.e., concentration of heavy ^{18}O) characterizing carbonates and fossil tests that precipitate at very low temperature (Friedman and O'Neil, 1977; Chacko et al., 2001; Hoefs, 2004). Volcanic and meteoric waters are characterized by strongly contrasting $\delta^{18}O$ values, being positive and negative, respectively. Quartz from metasedimentary rocks and S-type granites inherit a high-$\delta^{18}O$ supracrustal signature from the source, whereas quartz from hydrothermally altered rocks that have interacted with negative-$\delta^{18}O$ meteoric waters at high-temperature have low $\delta^{18}O$ (Bindeman, 2008).

In the Himalayan orogen, granitoid bodies in the Trans-Himalaya, North Himalaya, Greater Himalaya, and Lesser Himalaya have different isotopic bulk-rock ranging from ~6 ‰ for Trans-Himalayan batholiths to 14 ‰ for Greater Himalaya (Debon et al., 1986; Blattner et al., 1983; France-Lanord et al., 1988). Bulk-quartz and quartz-vein signatures in metasedimentary rocks range from 10 to 12 ‰ in the Lesser Himalaya to 12–14 ‰ in gneisses of the Greater Himalaya, and up to 21 ‰ in Tethys Himalayan carbonates (France-Lanord et al., 1988; Boullier et al., 1991; Evans et al., 2008, Fig. 1). Finally, hydrothermal circulation of meteoric water leads to ^{18}O depleted composition reaching negative values in extreme cases (Blattner et al., 1989) that however represent only a very minor source of quartz for river sediment.

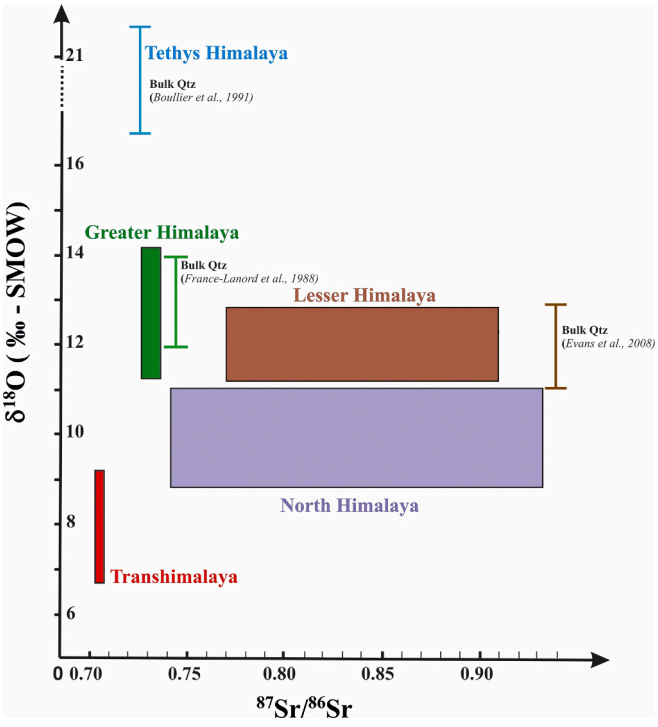

Fig. 1. The $\delta^{18}O$ and $^{87}Sr/^{86}Sr$ values of bulk rocks and/or river sediments (rectangle, data from Debon et al., 1986, France-Lanord et al., 1993; Singh and France-Lanord, 2002) and $\delta^{18}O$ of bulk quartz (line) derived from diverse Himalayan tectonic domains. $\delta^{18}O$ values expressed relative to standard mean ocean water, SMOW.

3. Materials and methods

3.1. Sample choice

Ten mono-source samples were considered as endmembers for this study: one suspended-load silt from the Marsyandi River; nine bank sands from rivers each draining a distinct Himalayan geological domain (Yigong and Parlung rivers representing theTrans-Himalaya, Khudi and Langtang rivers representing the Greater Himalaya, Paudi, Andi, and Anku rivers representing the Lesser Himalaya, Upper Marsyandi mostly representing the Tethys Himalaya but partly also the Greater Himalaya, and Miristi Khola sourced in the Annapurna Limestone). Multiple-source samples include five samples from selected rivers draining multiple sources (one suspended-load silt and one bank sand from from Narayani river, and one bedload sand from Siang, Ganga and Brahmaputra rivers) and seven Bengal Fan turbiditic samples ranging in age from Pleistocene to Miocene (Table 1, Fig. 2). Petrographic and heavy-mineral data are illustrated in Limonta et al. (2023) for Bengal Fan samples and in Garzanti et al. (2007) and Garzanti (2019b) for Himalayan river sands.

3.2. Sample preparation

After drying, ~15 g of each sample was separated by wet sieving into different phi classes. For SIMS analysis we considered the 5-phi-wide 15–500 μm fraction for Bengal Fan tubidites, the 5–500 μm fraction for suspended river sediments, and the 50–500 μm fraction for bedload river sediments (Supplementary Table A1). Quartz was pre-concentrated by separation with Na-polytungstate (Andò, 2020) followed by repeated dissolution in H_2SiF_6 and HCl to eliminate all mineral phases other than quartz (Lupker et al., 2017). For each sample, an aliquot of 5 mg of quartz was pressed in an indium plate and polished using 3 μm and 1 μm diamond paste on firm paper placed on a plain glass plate to minimize the relief difference between embedded quartz grains and enclosing indium matrix (Kita et al., 2009). After cleaning with Ethanol, the mounts were coated with ~40-nm-thick gold film and then stored for several hours in the 6-positions ion-microprobe sample-storage chamber under $\sim 10^{-8}$ mbar vacuum before the beginning of the analytical session. Quartz grains representing different samples were mounted in different sample holders to avoid any possible chance of fortuitous mixing.

3.3. SIMS analyses

The oxygen-isotope composition of quartz grains, from 71 to 207 of each of the 15 river-sediment samples and from the 7 Bengal Fan turbidite samples were analyzed by CAMECA IMS 1270 E7 ion microprobe in the Centre de Recherches Peétrographiques et Géochimiques (CRPG, Nancy, France).

The analyses were carried out using a focused and then rastered to 10 × 10 μm Cs^+ primary beam of 2–3 nA current. The $^{18}O/^{16}O$ isotopic ratios were analyzed in multi-collection mode using two off-axis, L'2 and H1 Faraday Cup (FC) detectors for counting simultaneously the respective $^{16}O^-$ and $^{18}O^-$ ion intensities. The FC gain was calibrated daily using the CAMECA built-in amplifier calibration routine, and the raw $^{16}O^-$ and $^{18}O^-$ ion signals were corrected for the real FC backgrounds signals measured during the pre-sputtering time before each measurement. The ion intensities obtained on the ^{16}O- and ^{18}O-peaks were ~ 2×10^9 cps and always higher than 10^6 cps, respectively. The Bresil2 ($\delta^{18}O_{V\text{-}SMOW}$ 20.3 ± 0.3 ‰), Sonar2 ($\delta^{18}O_{V\text{-}SMOW}$ 15.25 ± 0.3 ‰), and NL615 ($\delta^{18}O_{V\text{-}SMOW}$ 18.4 ± 0.2 ‰) CRPG internal quartz

Table 1
Key information on studied modern river sediments and Bengal Fan turbidites sampled during IODP Expedition 354.

River Sediments				
Samples	River	Latitude (N)	Longitude (E)	
TSA9	Yigong	30° 2′ 22.920″	95° 14′ 35.880″	Bedload
TSA8	Parlung	30° 7′ 27.480″	95° 3′ 8.640″	Bedload
CA964	Khudi	28° 20′ 56.832″	84° 19′ 53.436″	Bedload
CA10130	Langtang	28° 13′ 23.250″	85° 32′ 60.000″	Bedload
CA10118	Paudi	28° 6′ 40.968″	84° 25′ 36.408″	Bedload
MO270	Andi	28° 2′ 34.440″	83° 47′ 25.080″	Bedload
CA15002	Anku	27° 59′ 39.019″	84° 49′ 36.275″	Bedload
CA13161	Upper Marsyandi	28° 33′ 3.960″	84° 14′ 17.640″	Bedload
MA270615	Upper Marsyandi	28° 33′ 7.146″	84° 14′ 29.807″	Suspended Load
PB27	Miristi	28° 30′ 52.200″	83° 39′ 34.920″	Bedload
CA1010	Narayani	27° 43′ 29.579″	84° 25′ 40.033″	Bedload
SNGC1	Narayani	27° 41′ 58.200″	84° 25′ 8.400″	Suspended Load
BR1224	Siang	28° 14′ 9.600″	94° 59′ 53.520″	Bedload
BR706	Brahamaputra	24° 24′ 29.531″	89° 48′ 0.090″	Bedload
BR8252	Ganga	24° 3′ 14.040″	89° 1′ 29.640″	Bedload

Bengal fan turbidites								
Expedition	Hole	Latitude (N)	Longitude (E)	Water depth (m)	Core interval (m)	Recovery (%)	Age	n° samples
354	U1454B	8°0.4083	85°51.0025	3710	147.4	91.1 %	Calabrian-recent	1
354	U1450A	8°0.4201	87°40.2478	3655	444.7	64.0 %	Tortonian-recent	1
354	U1451A	8°0.4195	88°44.5012	3607	394.9	67.8 %	Tortonian-Chibanian	2
354	U1451B	8°0.4203	88°44.4745	3607	627.6	53.1 %	Oligocene	3

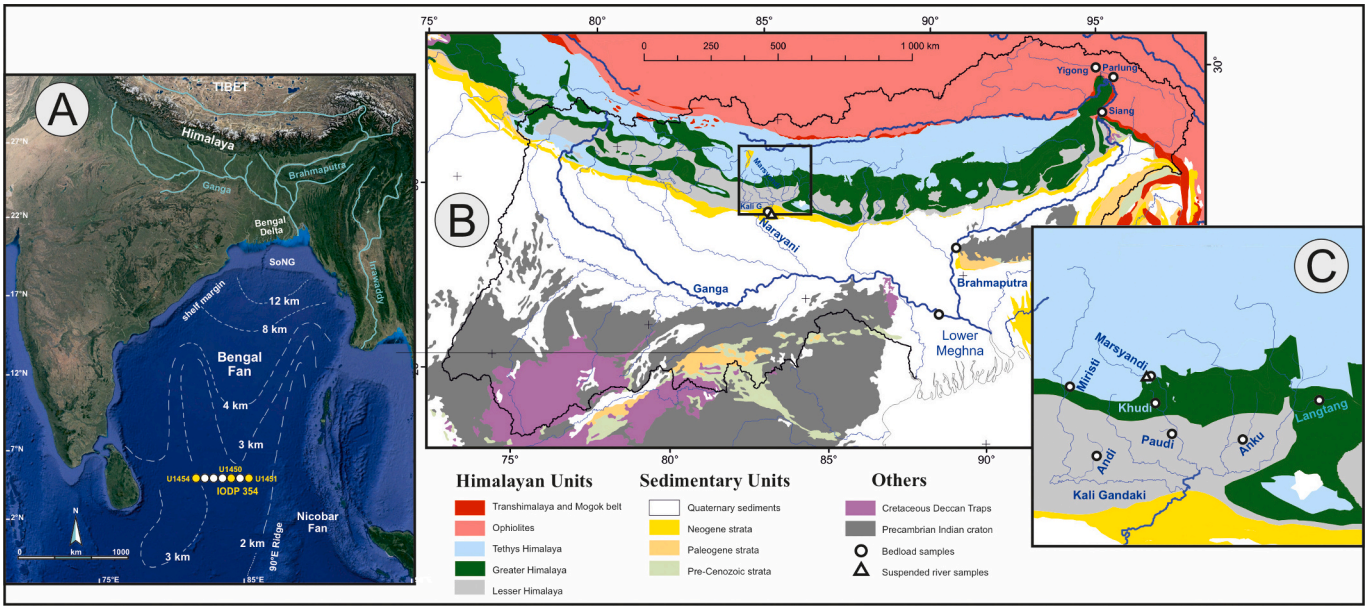

Fig. 2. A) Location map with studied IODP sites (yellow circles). B—C) Geological sketch map of Himalayas (mod. After Lenard, 2019) with location of analyzed river samples. (For interpretation of the references to colour in this figure legend, the reader is referred to the web version of this article.)

reference materials were employed to define instrumental mass fractionation (IMF) during SIMS measurements (Giuliani et al., 1998; Supplementary Fig. S1). Their oxygen-isotope compositions relative to V-SMOW were determined by multiple replicate measurements in the Stable Isotope Laboratory of CRPG using classic BrF_5 fluorination technique. In addition, one or more reference quartz grains or synthetic quartz glass were mounted together with the samples to: i) monitor instrumental drift during several consequent ~24-h-long uninterrupted analytical sub-sessions; and, ii) perform cross-calibration with a separate standard mount containing all employed reference quartz samples.

The analyses were performed during three separate analytical sessions (S1, S2, and S3 in May, June, and October 2023, one week for each session) using slightly different analytical conditions including fluctuations in primary beam current or vacuum pressure in the sample chamber. During session S1, we used only Bresil2 reference quartz, measured 5 to 6 times every 50 unknown quartz grain measurements. During sessions S2 and S3, we used Bresil2, Sonar2 and NL615 quartz standards, performing up to 5 replicate analyses of each at the beginning of sample measurements. Moreover, the NL615 reference quartz was analyzed 5–6 times every 50 measurements of the unknown quartz grains (Supplementary Table A2).

The SE internal precision (standard error of the mean based on the number of cycles in a single measurement, calculated as $SE = (\sigma / N^{0.5})$ where N is the number of observations, Valley et al., 2009) obtained on the reference quartz after ~150 s (30 cycles, 5 s per cycle) was better than 0.1 ‰. The external reproducibility (±1σ calculated from several

replicate measurements, typically 5 per standard) was ~0.3 ‰ obtained on the reference materials Bresil2, Sonar2, and NL615. The somewhat elevated internal uncertainty (up to ±0.4 ‰) observed preferentially during the analyses of unknown quartz grains is plausibly related to surface irregularities that remained after polishing quartz grains smaller than 100 μm.

To favor the analysis of larger number of grains over analytical precision and to do a statistical analysis of $\delta^{18}O$ data, we decreased the number of cycles in individual measurements from 30 cycles (session S1) to 10 cycles (in sessions S2 and S3). In the ideal case the precision decreases when reducing the number of cycles by a factor calculated as the ratio between the square root of 30 cycles (~5.47) and the square root of 10 cycles (~3.16), which is equal to 1.73. The average precision obtained using 30 cycles in the first session is 0.25 ± 0.04, whereas the precision obtained using 10 cycles is 0.41 ± 0.12 ‰ and 0.36 ± 0.10 ‰ in the second and third sessions, respectively. This basically corresponds to the above-calculated factor, namely 1.64 and 1.44 for the second and the third sessions, respectively. The deviation of these values from the "theoretical" one is apparently due to the error contribution incurred during the replicated measurements of the used reference quartz. It is worth emphasizing that we used 30 cycles in the first session and 10 cycles in the second and the third ones aiming to compare how this reduction (a) affects the analytical precision of the measurements and (b) still allows us to achieve the goal of our study by increasing the number of unknown quartz grain measurements. The precision of 10 cycles is acceptable for this study because the difference of $\delta^{18}O$ in Himalayan endmembers is higher than 1 ‰.

The measured $^{18}O/^{16}O$ ratios were converted to delta values ($\delta^{18}O_{RAW}$, given in ‰) by normalizing them to $^{18}O/^{16}O$ of Standard Mean Ocean Water ($(^{18}O/^{16}O)_{VSMOW} = 0.0020520$; Craig, 1961; Baertschi, 1976) according the equation:

$$\delta^{18}O_{RAW} = 1000 \times \left[\left({}^{18}O/{}^{16}O \right)_{RAW} \Big/ \left({}^{18}O/{}^{16}O_{VSMOW} - 1 \right) \right] \quad (1)$$

Instrumental mass fractionation (IMF or mass bias) values are defined as:

$$\delta^{18}O_{IMF} = \delta^{18}O_{STD-RAW} - \delta^{18}O_{STD-TRUE} \quad (2)$$

where STD-RAW and STD-TRUE denote the raw (measured) and true $\delta^{18}O$ values of the used quartz standards, which were determined based on the measurements performed before each analytical session. The raw $\delta^{18}O$ obtained for the unknown quartz samples were converted to their true values, using the determined IMF values according to the equation:

$$\delta^{18}O_{TRUE} = \delta^{18}O_{RAW} - \delta^{18}O_{IMF} \quad (3)$$

3.4. Data processing

Oxygen-isotope ratios were determined for ~3900 quartz grains (data reported in Supplementary Tables A3-A4). For each sample, $\delta^{18}O$ values are presented as a histogram with predefined classes from 5 ‰ to 25 ‰ with bin 1 ‰. The *OriginPro* software was employed to fit the histogram with a Gaussian curve and calculate the peak height, peak position, and peak width of the distribution (Supplementary Fig. S2a). Gaussian deconvolution allowed us to identify different sub-populations in multimodal sediment samples (Supplementary Fig. S2b). For multi-sourced samples, the deconvolution procedure was the same as for the endmembers with the exception of peak position which was fixed using values defined from endmembers. Goodness of fit was evaluated by R^2 values that range from 0.934 to 0.996. The quartz contribution from different endmembers to mixed Ganga, Brahmaputra, and Bengal Fan samples was calculated based on the relative area of each Gaussian component.

4. Results

Single grain data are represented as histograms combining samples with similar sources in Fig. 3. Grains of the Parlung and Yigong rivers draining Trans-Himalaya batholiths exhibit a single dominant population at 11.5 ‰ (dominant peak resulting from the fitting approach). The Upper Marsyandi River mostly sourced from the Tethys Himalaya is characterized by the highest $\delta^{18}O$ values, ranging from 16 ‰ to 25 ‰. Its population at 14.5 ‰ is similar to that of Langtang and Khudi rivers (at 14.3 ‰) draining the Greater Himalaya which is exposed also in the lower part of the Upper Marsyandi basin. The Khudi and Langtang rivers draining the Greater Himalaya show $\delta^{18}O$ values peaking around 14.9 ‰ and 13.1 ‰ respectively (Supplementary Fig. S3). Quartz grains from the Paudi, Anku, and Andi Rivers draining the Lesser Himalaya display a main population at 11.5 ‰, with a minor populations at 8.2 ‰ and 14.6 ‰ (Fig. 3a).

Both suspended-load silt and bedload sand of the Narayani River display a polymodal distribution with $\delta^{18}O$ populations at 12.0 ‰, 14.0 ‰, 18.2 ‰, and 22.2 ‰. Ganga sand shows $\delta^{18}O$ populations at 12.4 ‰, 14.5 ‰, and 16.7 ‰. Sand in the Siang River and in the Brahmaputra River downstream exhibit a major population at ~11 ‰ and a minor one at ~14.4 ‰; Brahmaputra sand displays a further population at 20.5 ‰ (Fig. 3b).

In Bengal Fan turbidite samples, the distribution of $\delta^{18}O$ values ranges from 5 ‰ to 25 ‰, with a main population around 12 ‰, associated in some samples with a population at 14.3 ‰, and with an invariably minor population around 18 ‰ (Fig. 3c) independently of grain size (Supplementary Fig. S5).

5. Discussion of the results and validation of the method

Given the abundant and widespread occurrence of quartz in siltstones and sandstones, the single-grain technique illustrated in this article can be applied to identify provenance of any silt- to sand-sized sediment derived from igneous, metamorphic and sedimentary domains. Wherever the $\delta^{18}O$ fingerprints of quartz grains from endmember sources are sufficiently distinct, the relative supply from different domains to sedimentary deposits can be effectively quantified, thus complementing traditional approaches.

This proves to be the case in Himalayan-derived sediments, where endmember geological units contain quartz with $\delta^{18}O$ signature ranging from as low as 5 ‰ for Trans-Himalayan batholiths to as high as 25 ‰ for the Tethys Himalayan Zone. The great potential of the new approach resides in the possibility to quantify Tethys Himalayan contribution distinguished by very high $\delta^{18}O$ values.

The Lesser Himalaya and Trans-Himalaya are characterized by lower $\delta^{18}O$ values than the Greater Himalaya and Tethys Himalaya, although there are significant overlaps, making it challenging to distinguish their relative contributions to the Brahamputra-Ganga-Bengal sedimentary system. For this reason, unlike for the Tethys Himalaya, the novel method does not allow us to distinguish Trans-Himalayan sources from Lesser Himalayan sources.

The Greater Himalaya supply a similar amount of quartz to Ganga and Brahmaputra sediments (~20 %), whereas the Tethys Himalaya contribution resulted to be markedly different (15 and 4 %, respectively), consistently with petrographic and mineralogical data (Garzanti, 2019b). The two rivers also show different amounts of sediments derived from Lesser Himalaya and Trans-Himalaya, respectively.

Single-grain $\delta^{18}O$ values characterizing Ganga sediments indicate a high quartz contribution from Greater Himalaya and Lesser Himalaya, consistently with Sr—Nd isotopic composition (Galy and France-Lanord, 2001). Quartz in the Narayani river resulted to be derived 20 % from the Lesser Himalaya and 8 % from the Tethys Himalaya. The relationship between quartz and carbonate of the Tethys is a complex problem linked to the degree of carbonate dissolution during erosion and quartz fertility of the Tethys formations. It appears contradictory that fraction of Tethys

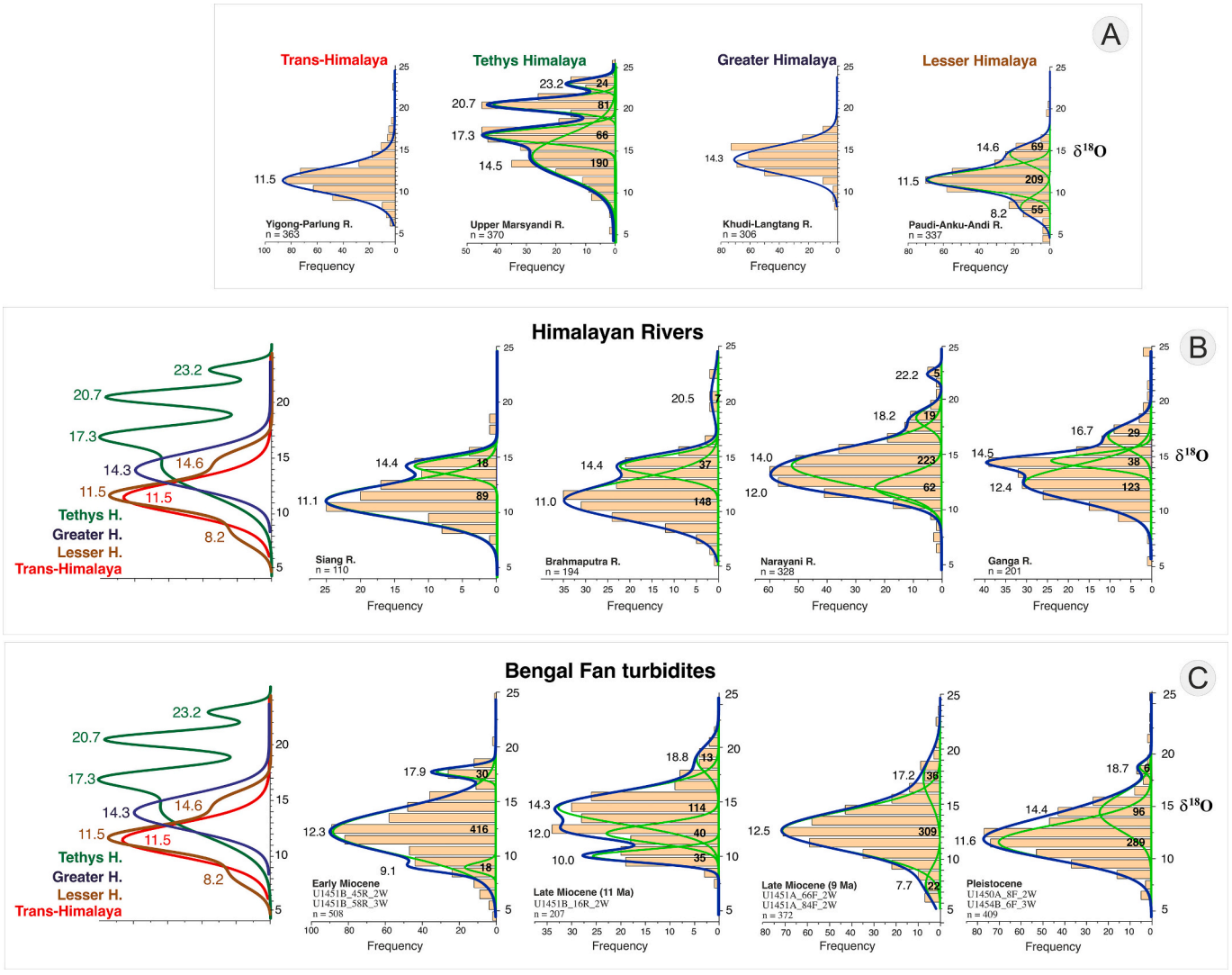

Fig. 3. A) $\delta^{18}O$ distribution in quartz grains of fluvial samples from endmember sources (Lesser Himalaya, Greater Himalaya, Tethys Himalaya and Trans-Himalaya. B) $\delta^{18}O$ distribution in quartz grains in sand of multi-source Siang, Brahmaputra, Narayani and Ganga rivers. C) $\delta^{18}O$ distribution in quartz grains from Bengal Fan turbidite samples ranging in age from Miocene to Pleistocene. Detailed $\delta^{18}O$ distribution in quartz grains of each Bengal fan turbiditic sample is shown in Supplementary Fig. S4. ($\delta^{18}O$ values expressed relative to standard mean ocean water, SMOW; n = number of analyzed quartz grains, the area of the density curve are indicated in bold).

derived quartz is higher in the Ganga than in the Narayani as the Narayani drains the largest proportion of Tethys Himalaya and carries the highest proportion of detrital carbonates of all Ganga's tributaries (Lupker et al., 2012; Morin et al., 2018). In detail, bedload and suspended load samples of Narayani river reflect contrasted carbonate contents of 8.5 and 13 wt% for Tethys's quartz contribution of 12 and 20 %, respectively. In comparison, the Ganga sample carries only 3.5 % of carbonate for 15 % of Tethys quartz (Fig. 4). This contrast likely derives from carbonate dissolution during transport.

Single-grain $\delta^{18}O$ values of Bengal Fan turbidites display a dominant population between 11.0 ‰ and 11.5 ‰. The very same population characterizes the Yigong and Parlung rivers draining the Trans-Himalayan domain in the Eastern Himalayan Syntaxis, as well as the Siang and Brahmaputra rivers downstream. This fully supports the prominent supply from the Trans-Himalayan to the Siang and Brahmaputra Rivers and Bengal Fan, already documented by elemental and isotope geochemistry (Singh and France-Lanord, 2002), petrography and heavy minerals (Garzanti et al., 2004, 2019b), and detrital geochronology (U—Pb zircon: Lang and Huntington, 2014; Dong et al., 2023; U—Pb rutile: Govin et al., 2020; $^{40}Ar/^{39}Ar$ mica: Gemignani et al., 2018; zircon fission tracks: Enkelmann et al., 2011).

All Bengal Fan turbidites show a minor proportion of quartz grains with $\delta^{18}O$ values >16 ‰, related to Tethys Himalayan contribution to deep-sea sediments. The magnitude of this peak decreases from Miocene to Pleistocene turbidites (Fig. 3c), suggesting a decreasing supply from Tethys Himalaya supply decreasing from 7 % to 2 %. The maximum percentage of Tethys Himalayan detritus is identified in Upper Miocene strata, which is supported by the positive correlation between the percentage of carbonate content and the percentage of $\delta^{18}O$ values >16 ‰ in turbidites (Fig. 4). This fully supports more significative supply from the Tethys Himalaya to Bengal Fan during the Late and Middle Miocene than during the Pliocene-Pleistocene, already documented by the higher detrital carbonate content of the Upper and Middle Miocene turbidites (Ryb et al., 2024; France-Lanord et al., 2016). No relationship is observed instead between Sr—Nd values and single-grain quartz $\delta^{18}O$ values (Supplementary Figure S6ab).

5.1. *Limitations of the single quartz $\delta^{18}O$ method*

The relative sediment contribution from two sources with distinct

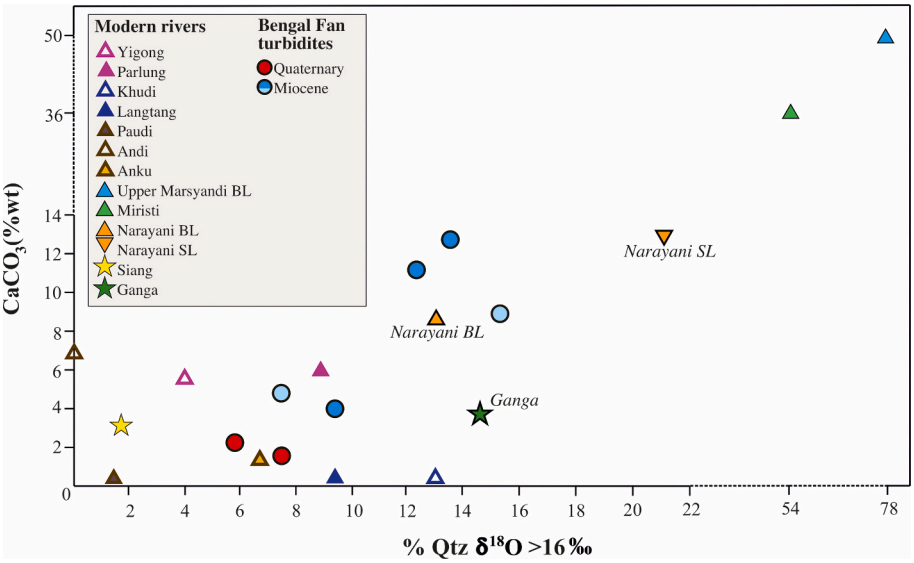

Fig. 4. Positive correlation between the percentage of quartz grains with $\delta^{18}O > 16$ ‰ and percentages of carbonate content: both provenance proxies decrease from Miocene to Pleistocene strata of Bengal Fan (indicated with circles). Data of modern rivers are reported for comparison (indicated with triangles and stars).

isotopic fingerprints can be assessed accurately, but where detritus is derived from multiple tectonic domains with overlapping isotopic signatures, as commonly is the case in orogenic settings and large river-turbidite systems, then single isotopic ratios may give equivocal responses serving at best to check provenance estimates made with other independent methods (e.g., Clift et al., 2002; Padoan et al., 2011). This is the case for all isotopic ratios (e.g., $^{87}Sr/^{86}Sr$, $^{143}Nd/^{144}Nd$) used to discriminate contributions from different sources, because different combinations of primary signals may produce the same result giving rise to undetermined interpretations.

In our case, similar $\delta^{18}O$ values are shared by different Himalayan domains. In particular, quartz grains from the Trans-Himalaya and Lesser Himalaya show a wide range of overlapping $\delta^{18}O$ values, making it challenging to distinguish their relative contributions to the Bengal Fan. Quartz characterized by $\delta^{18}O$ values of ~11 ‰ can be safely related to the Lesser Himalaya in the case of the Ganga River, which does not drain the Trans-Himalaya, whereas it is chiefly derived from Trans-Himalayan granitoids rapidly eroded in the Eastern Himalayan Syntaxis in the case of the Siang-Brahmaputra River. In other cases, integrating isotopic data with geological insight and parameters offering complementary information is required to enhance the accuracy of provenance analysis.

Moreover, quartz grains in Bengal Fan turbidites are derived in unknown but possibly significant proportion from recycling of siliciclastic deposits with high sand-generation potential (e.g., Siwalik Group; Szulc et al., 2006; Govin et al., 2018; Garzanti, 2019b). The problem of recycling is hard to solve with any mineralogical or isotopic method including $\delta^{18}O$, which can nevertheless identify the original source (protosource) of quartz grains in case of limited diagenetic modification.

Despite such difficulties, common to all methods, investigating quartz is indispensable, because quartz constitutes the majority of orogenic sediment. Zircon is widely targeted in detrital-geochronology studies, and yet it is much rarer, accounting on average for only ~1 out of 5000 grains (Garzanti and Andò, 2007); provenance analysis cannot be limited to such a minimal fraction of the sediment flux (Garzanti et al., 2018). Moreover, zircon has a much narrower grain-size distribution compared to quartz (mostly <250 μm), and small zircons cannot be dated with the widely used techniques whereas quartz grains can be analyzed in the whole size spectrum from fine silt to pebble. A similar problem is encountered for Nd isotopes, because the Nd budget in siliciclastic sediment is controlled by a limited number of rare minerals (generally monazite; Garçon et al., 2014; Garzanti et al., 2022), derived from very specific source rocks (e.g., pegmatites; Spear and Pyle, 2002; Garzanti et al., 2024). A strong fertility problem is associated with studies focusing directly or indirectly on rare minerals such as zircon or monazite (Malusà et al., 2016), which is not the case for quartz oxygen-isotope studies.

Because all methods have limitations, multi-method approaches are the only way to overcome ambiguous information from the sedimentary record, and the quartz $\delta^{18}O$ method outlined here can provide useful complementary information to any provenance study.

6. Conclusions

The oxygen-isotope signature of single quartz grains represents a new promising tool to determine the provenance of quartz grains. Because quartz represents a large majority of siliciclastic sediment generated in cratonic as well as in orogenic settings, this is a fundamental task that has not yet been accomplished by any other method with full success. In this study, the $\delta^{18}O$ signatures of single quartz grains has been determined by ion microprobe LG-SIMS in sediments carried by rivers draining different Himalayan domains and in Bengal fan turbidites. The $\delta^{18}O$ fingerprint of different Himalayan source-rock domains are clearly distinguished in sediments independently of their grain size, ranging from as low as 5 ‰ for Trans-Himalayan batholiths exposed in the Eastern Himalayan Syntaxis to as high as 25 ‰ for sedimentary rocks of the Tethys Himalayan Zone. Significant overlap around $\delta^{18}O$ values of 11 ‰, however, is shown by quartz grains derived from both Trans-Himalayan and Lesser Himalayan sources. Geological information allows to distinguish these two provenances in the case of the Ganga River, which does not drain the Trans-Himalayan domain, or the Siang-Brahmaputra River, which is instead chiefly derived from the Eastern Himalayan Syntaxis, but the issue cannot be resolved in the case of Bengal Fan turbidites.

Common single-grain techniques consider accessory minerals like zircon, but investigating the provenance of quartz grains is quantitatively far more significant, considering that quartz is more than three-orders-of-magnitude more abundant than zircon in sediments, and occurs and can be analyzed in a far larger grain-size range than zircon. Traditional approaches to determine quartz origin, including petrography and cathodo-luminescence, have obtained limited success. The $\delta^{18}O$ method proposed here can be profitably applied in any sediment-provenance study as a precious complement to classical methods applied to the same quartz grains (e.g. trace elements, cathodo-

luminiscence, OH-defects, and petrographic characteristics) and classic techniques (e.g., petrography, heavy minerals, elemental geochemistry, isotope geochemistry) to discriminate detrital quartz derived from felsic igneous, metamorphic, or sedimentary domains.

Supplementary data to this article can be found online at https://doi.org/10.1016/j.chemgeo.2024.122525.

CRediT authorship contribution statement

Mara Limonta: Writing – review & editing, Writing – original draft, Visualization, Validation, Software, Methodology, Investigation, Funding acquisition, Formal analysis, Data curation, Conceptualization. **Christian France-Lanord:** Writing – review & editing, Supervision, Resources, Project administration, Methodology, Funding acquisition, Conceptualization. **Albert Galy:** Writing – review & editing, Funding acquisition. **Andrey Gurenko:** Writing – review & editing, Investigation. **Nordine Bouden:** Investigation. **Eduardo Garzanti:** Writing – review & editing.

Declaration of competing interest

The authors declare that they have no known competing financial interests or personal relationships that could have appeared to influence the work reported in this paper.

Acknowledgments

The studied Bengal Fan samples were obtained thanks to the International Ocean Discovery Program (IODP) and the kind help of Dr. Kubo and the technical staff of IODP Core Repository Kochi Institute for Core Sample Research (http://www.kochi-core.jp/en/iodp-curation/index.html). This research was funded through ECORD-IODP-France postdoc fellowship and ANR Himal Fan and GiNoha. We thank Editor Dr. S. Aulbach and reviewers Prof. E. Le Pera and PhD J. Schönig for their constructive comments.

Data availability

Data will be made available on request.

References

Ackerson, M.R., Tailby, N.D., Watson, E.B., 2015. Trace elements in quartz shed light on sediment provenance. Geochem. Geophys. Geosyst. 16, 1894–1904. https://doi.org/10.1002/2015GC005896.

Aitken, M.J., 1985. Thermoluminescent Dating. Academic Press, London, p. 359.

Aitken, M.J., 1998. An Introduction to Optical Dating. The Dating of Quaternary Sediments by the Use of Photon-Stimulated Luminescence. Oxford University Press, Oxford, p. 267.

Aléon, J., Chaussidon, M., Marty, B., Schütz, L., Jaenicke, R., 2002. Oxygen isotopes in single micrometer-sized quartz grains: tracing the source of Saharan dust over long-distance atmospheric transport. Geochim. Cosmochim. Acta 66 (19), 3351–3365.

Andò, S., 2020. Gravimetric separation of heavy minerals in sediments and rocks. Minerals 10 (3), 273.

Augustsson, C., Reker, A., 2012. Cathodoluminescence spectra of quartz as provenance indicators revisited. J. Sediment. Res. 82 (8), 559–570.

Augustsson, C., Aehnelt, M., Voigt, T., Kunkel, C., Meyer, M., Schellhorn, F., 2019. Quartz and zircon decoupling in sandstone: Petrography and quartz cathodoluminescence of the early Triassic continental Buntsandstein Group in Germany. Sedimentology 66 (7), 2874–2893.

Baertschi, P., 1976. Absolute ^{18}O content of standard mean ocean water. Earth Planet. Sci. Lett. 31 (3), 341–344.

Baron, M.A., Stalder, R., Konzett, J., Hauzenberger, C.A., 2015. OH-point defects in quartz in B-and Li-bearing systems and their application to pegmatites. Phys. Chem. Miner. 42, 53–62.

Basu, A., 1985. Reading provenance from detrital quartz. In: Zuffa, G.G. (Ed.), Provenance of Arenites. Springer Netherlands, Dordrecht, pp. 231–247.

Bernet, M., Bassett, K., 2005. Provenance analysis by single-quartz-grain SEM-CL/optical microscopy. J. Sediment. Res. 75 (3), 492–500.

Bernet, M., Kapoutsos, D., Bassett, K., 2007. Diagenesis and provenance of Silurian quartz arenites in South-Eastern New York State. Sediment. Geol. 201 (1–2), 43–55.

Bindeman, I., 2008. Oxygen isotopes in mantle and crustal magmas as revealed by single crystal analysis. Rev. Mineral. Geochem. 69 (1), 445–478.

Blatt, H., 1967a. Original characteristics of clastic quartz grains. J. Sediment. Res. 37 (2), 401–424.

Blatt, H., 1967b. Provenance determinations and recycling of sediments. J. Sediment. Res. 37 (4), 1031–1044.

Blatt, H., 1987. Perspectives: oxygen isotopes and the origin of quartz. J. Sediment. Res. 57 (2), 373–377.

Blatt, H., Middleton, G., Murray, R., 1980. Origin of Sedimentary Rocks, 2nd edn. Prentice-Hall, Englewood Cliffs, NJ.

Blattner, P., Dietrich, V., Gansser, A., 1983. Contrasting ^{18}O enrichment and origins of High Himalayan and Transhimalayan intrusives. Earth Planet. Sci. Lett. 65 (2), 276–286.

Blattner, P., Cheng-Wei, J., Yong, X., 1989. Oxygen isotopes in mantle related and geothermally altered magmatites of the Transhimalayan (Gangdese) ranges. Contrib. Mineral. Petrol. 101, 438–446.

Boggs Jr., S., Kwon, Y.I., Goles, G.G., Rusk, B.G., Krinsley, D., Seyedolali, A., 2002. Is quartz cathodoluminescence color a reliable provenance tool? A quantitative examination. J. Sediment. Res. 72 (3), 408–415.

Bokman, J.W., 1952a. Clastic quartz particles as indices of provenance. J. Sediment. Res. 22 (1), 17–24.

Bokman, J.W., 1952b. Clastic quartz particles as indices of provenance. J. Sediment. Res. 22 (1), 17–24.

Boullier, A.M., France-Lanord, C., Dubessy, J., Adamy, J., Champenois, M., 1991. Linked fluid and tectonic evolution in the High Himalaya mountains (Nepal). Contrib. Mineral. Petrol. 107, 358–372.

Breiter, K., Ackerman, L., Svojtka, M., Müller, A., 2013. Behavior of trace elements in quartz from plutons of different geochemical signature: a case study from the Bohemian Massif, Czech Republic. Lithos 175–176, 54–67.

Capaldi, T.N., Rittenour, T.M., Nelson, M.S., 2022. Downstream changes in quartz OSL sensitivity in modern river sand reflects sediment source variability: Case studies from Rocky Mountain and Andean rivers. Quat. Geochronol. 71, 101317.

Carter, N.L., Christie, J.M., Griggs, D.T., 1964. Experimental deformation and recrystallization of quartz. J. Geol. 72 (6), 687–733.

Chacko, T., Cole, D.R., Horita, J., 2001. Equilibrium oxygen, hydrogen and carbon isotope fractionation factors applicable to geologic systems. Rev. Mineral. Geochem. 43 (1), 1–81.

Chang, Z., Zhou, L., 2019. Evidence for provenance change in deep sea sediments of the Bengal Fan: a 7 million year record from IODP U1444A. J. Asian Earth Sci. 186, 104008.

Clayton, R.N., Epstein, S., 1958. The relationship between O18/O16 ratios in coexisting quartz, carbonate, and iron oxides from various geological deposits. J. Geol. 66 (4), 345–371.

Clayton, R.N., Epstein, S., 1961. The use of oxygen isotopes in high-temperature geological thermometry. J. Geol. 69 (4), 447–452.

Clayton, R.N., Rex, R.W., Syers, J.K., Jackson, M.L., 1972. Oxygen isotope abundance in quartz from Pacific pelagic sediments. J. Geophys. Res. 77 (21), 3907–3915.

Clayton, R.N., Jackson, M.L., Sridhar, K., 1978. Resistance of quartz silt to isotopic exchange under burial and intense weathering conditions. Geochim. Cosmochim. Acta 42 (10), 1517–1522.

Clift, P.D., Lee, J.I., Hildebrand, P., Shimizu, N., Layne, G.D., Blusztajn, J., Blum, J.D., Garzanti, E., Khan, A.A., 2002. Nd and Pb isotope variability in the Indus River System: implications for sediment provenance and crustal heterogeneity in the Western Himalaya. Earth Planet. Sci. Lett. 200 (1–2), 91–106.

Craig, H., 1961. Isotopic variations in meteoric waters. Science 133 (3465), 1702–1703.

Debon, F., Fort, P.L., Sheppard, S.M., Sonet, J., 1986. The four plutonic belts of the Transhimalaya-Himalaya: a chemical, mineralogical, isotopic, and chronological synthesis along a Tibet-Nepal section. J. Petrol. 27 (1), 219–250.

Dong, X., Hu, X., Garzanti, E., Liang, W., Li, G., Lai, W., Wang, C., Han, Z., Deng, T., Li, Z., 2023. The extraordinary Namche Barwa sediment factory in the Eastern Himalayan Syntaxis. Basin Res. 35 (6), 2193–2216.

Dott, R.H., 2003. The importance of eolian abrasion in supermature quartz sandstones and the paradox of weathering on vegetation-free landscapes. J. Geol. 111 (4), 387–405.

Enkelmann, E., Ehlers, T.A., Zeitler, P.K., Hallet, B., 2011. Denudation of the Namche Barwa antiform, eastern Himalaya. Earth Planet. Sci. Lett. 307 (3–4), 323–333.

Evans, M.J., Derry, L.A., France-Lanord, C., 2008. Degassing of metamorphic carbon dioxide from the Nepal Himalaya. Geochem. Geophys. Geosyst. 9 (4).

Folk, R.L., 1980. Petrology of Sedimentary Rocks. Hemphill Publishing Co., Austin (USA), p. 184.

France-Lanord, C., Sheppard, S.M., Le Fort, P., 1988. Hydrogen and oxygen isotope variations in the High Himalaya peraluminous Manaslu leucogranite: evidence for heterogeneous sedimentary source. Geochim. Cosmochim. Acta 52 (2), 513–526.

France-Lanord, C., Derry, L., Michard, A., 1993. Evolution of the Himalaya since Miocene time: isotopic and sedimentologic evidence from the Bengal Fan. In: Treloar, P.J., Searle, M. (Eds.), Himalayan Tectonics Geological Society Special Publication, pp. 603–621, 74 London.

France-Lanord, C., Spiess, V., Klaus, A., Adhikari, R.R., Adhikari, S.K., Bahk, J.-J., Baxter, A.T., Cruz, J.W., Das, S.K., Dekens, P., Duleba, W., Fox, L.R., Galy, A., Galy, V., Ge, J., Gleason, J.D., Gyawali, B.R., Huyghe, P., Jia, G., Lantzsch, H., Manoj, M.C., Martin, Y.M., Meynadier, L., Najman, Y.M.R., Nakajima, A., Ponton, C., Reilly, B.T., Rogers, K.G., Savian, J.F., Schwenk, T., Selkin, P.A., Weber, M.E., Williams, T., Yoshida, K., 2016. Site U1451. In: Proceedings of the International Ocean Discovery Program, 354. https://doi.org/10.14379/iodp.proc.354.105.2016.

Friedman, I., O'Neil, J.R., 1977. In: Chapter, K.K. (Ed.), Data of Geochemistry: Compilation of Stable Isotope Fractionation Factors of Geochemical Interest, vol. 440. US Government Printing Office.

Frigo, C., Stalder, R., Hauzenberger, C.A., 2016. OH defects in quartz in granitic systems doped with spodumene, tourmaline and/or apatite: experimental investigations at 5–20 kbar. Phys. Chem. Miner. 43, 717–729.
Galy, A., France-Lanord, C., 2001. Higher erosion rates in the Himalaya: geochemical constraints on riverine fluxes. Geology 29 (1), 23–26.
Garçon, M., Chauvel, C., France-Lanord, C., Limonta, M., Garzanti, E., 2014. Which minerals control the Nd–Hf–Sr–Pb isotopic compositions of river sediments? Chem. Geol. 364, 42–55.
Garzanti, E., 2017. The maturity myth in sedimentology and provenance analysis. J. Sediment. Res. 87 (4), 353–365.
Garzanti, E., 2019a. Petrographic classification of sand and sandstone. Earth Sci. Rev. 192, 545–563.
Garzanti, E., 2019b. The Himalayan Foreland Basin from collision onset to the present: a sedimentary–petrology perspective. Geol. Soc. Lond. Spec. Publ. 483 (1), 65–122.
Garzanti, E., Andò, S., 2007. Heavy mineral concentration in modern sands: implications for provenance interpretation. Dev. Sedimentol. 58, 517–545.
Garzanti, E., Brignoli, G., 1989. Low temperature metamorphism in the Zanskar sedimentary nappes (NW Himalaya, India). Eclogae Geol. Helv. 82 (2), 669–684.
Garzanti, E., Vezzoli, G., Andò, S., France-Lanord, C., Singh, S.K., Foster, G., 2004. Sand petrology and focused erosion in collision orogens: the Brahmaputra case. Earth Planet. Sci. Lett. 220 (1–2), 157–174.
Garzanti, E., Vezzoli, G., Andò, S., Lavé, J., Attal, M., France-Lanord, C., DeCelles, P., 2007. Quantifying sand provenance and erosion (Marsyandi river, Nepal Himalaya). Earth Planet. Sci. Lett. 258 (3–4), 500–515.
Garzanti, E., Limonta, M., Vezzoli, G., An, W., Wang, J.G., Hu, X.M., 2018. Petrology and multimineral fingerprinting of modern sand generated from a dissected magmatic arc (Lhasa River, Tibet). In: Ingersoll, R.V., Lawton, T.F., Graham, S.A. (Eds.), Tectonics, Sedimentary Basins, and Provenance: A Celebration of William R. Dickinson's Career. Geological Society of America, pp. 197–221. https://doi.org/10.1130/2018.2540(09). Special Paper 540.
Garzanti, E., Vermeesch, P., Vezzoli, G., Andò, S., Botti, E., Limonta, M., Dinis, P., Hahn, A., Baudet, D., De Grave, J., Yaya, N.K., 2019a. Congo River sand and the equatorial quartz factory. Earth Sci. Rev. 197, 102918.
Garzanti, E., Vezzoli, G., Andò, S., Limonta, M., Borromeo, L., France-Lanord, C., 2019b. Provenance of Bengal Shelf Sediments: 2. Petrology and geochemistry of sand. Minerals 9 (10), 642.
Garzanti, E., Bayon, G., Vermeesch, P., Barbarano, M., Pastore, G., Resentini, A., Dennielou, B., Jouet, G., 2022. The Zambezi deep-sea fan: mineralogical, REE, Zr/Hf, Nd-isotope, and zircon-age variability in feldspar-rich passive-margin turbidites. J. Sediment. Res. 92 (11), 1022–1043.
Garzanti, E., Bayon, G., Barbarano, M., Resentini, A., Vezzoli, G., Pastore, G., Levacher, M., Adeaga, O., 2024. Anatomy of Niger and Benue river sediments from clay to granule: Grain-size dependence and provenance budget. J. Sediment. Res. https://doi.org/10.2110/jsr.2024.024.
Gemignani, L., Van der Beek, P.A., Braun, J., Najman, Y., Bernet, M., Garzanti, E., Wijbrans, J.R., 2018. Downstream evolution of the thermochronologic age signal in the Brahmaputra catchment (eastern Himalaya): Implications for the detrital record of erosion. Earth Planet. Sci. Lett. 499, 48–61.
Giuliani, G., France-Lanord, C., Coget, P., Schwarz, D., Cheilletz, A., Branquet, Y., Giard, D., Matin-Izard, P., Alexandrov, P., Piat, D.H., 1998. Oxygen isotope systematics of emerald: relevance for its origin and geological significance. Mineral. Deposita 33, 513–519.
Götze, J., 2012. Application of cathodoluminescence microscopy and spectroscopy in geosciences. Microsc. Microanal. 18 (6), 1270–1284.
Götze, J., Möckel, R. (Eds.), 2012. Quartz: Deposits, Mineralogy and Analytics. Verlag, Heidelberg, Springer. https://doi.org/10.1007/978-3-642-22161-3.
Götze, J., Plötze, M., 1997. Investigation of trace-element distribution in detrital quartz by Electron Paramagnetic Resonance (EPR). Eur. J. Mineral. 9 (3), 529–537.
Götze, J., Plötze, M., Habermann, D., 2001. Origin, spectral characteristics and practical applications of the cathodoluminescence (CL) of quartz–a review. Mineral. Petrol. 71, 225–250.
Götze, J., Plötze, M., Graupner, T., Hallbauer, D.K., Bray, C.J., 2004. Trace element incorporation into quartz: a combined study by ICP-MS, electron spin resonance, cathodoluminescence, capillary ion analysis, and gas chromatography. Geochim. Cosmochim. Acta 68 (18), 3741–3759.
Götze, J., Pan, Y., Müller, A., 2021. Mineralogy and mineral chemistry of quartz: a review. Mineral. Mag. 85 (5), 639–664.
Govin, G., Najman, Y., Dupont-Nivet, G., Millar, I., van Der Beek, P., Huyghe, P., O'Sullivan, P., Mark, C., Vögeli, N., 2018. The tectonics and paleo-drainage of the easternmost Himalaya (Arunachal Pradesh, India) recorded in the Siwalik rocks of the foreland basin. Am. J. Sci. 318 (7), 764–798.
Govin, G., van Der Beek, P., Najman, Y., Millar, I., Gemignani, L., Huyghe, P., Dupont-Nivet, G., Bernet, M., Mark, C., Wijbrans, J., 2020. Early onset and late acceleration of rapid exhumation in the Namche Barwa syntaxis, eastern Himalaya. Geology 48 (12), 1139–1143.
Heck, P.R., Huberty, J.M., Kita, N.T., Ushikubo, T., Kozdon, R., Valley, J.W., 2011. SIMS analyses of silicon and oxygen isotope ratios for quartz from Archean and Paleoproterozoic banded iron formations. Geochim. Cosmochim. Acta 75 (20), 5879–5891.
Hoefs, J., 2004. Stable Isotope Geochemistry, 5th edn. Springer-Verlag Berlin Heidelberg.
Hooker, J.N., Laubach, S.E., 2007. The geologic history of quartz grains, as revealed by color SEM-CL: Gulf Coast Association of Geological Societies. Transactions 57, 375–386.
Jacamon, F., Larsen, R.B., 2009. Trace element evolution of quartz in the charnockitic Kleivan granite, SW-Norway: the Ge/Ti ratio of quartz as an index of igneous differentiation. Lithos 107 (3–4), 281–291.
Jaeger, D., Stalder, R., Masago, H., Strasser, M., 2019. OH defects in quartz as a provenance tool: application to fluvial and deep marine sediments from SW Japan. Sediment. Geol. 388, 66–80.
Jeong, G.Y., Choi, J.H., 2012. Variations in quartz OSL components with lithology, weathering and transportation. Quat. Geochronol. 10, 320–326.
Kelly, S.D., Hesterberg, D., Ravel, B., 2008. Analysis of soils and minerals using X-ray absorption spectroscopy. Methods Soil Anal. 5 5, 387–463.
Kita, N.T., Ushikubo, T., Fu, B., Valley, J.W., 2009. High precision SIMS oxygen isotope analysis and the effect of sample topography. Chem. Geol. 264 (1–4), 43–57.
Knauth, L.P., Epstein, S., 1976. Hydrogen and oxygen isotope ratios in nodular and bedded cherts. Geochim. Cosmochim. Acta 40 (9), 1095–1108.
Lang, K.A., Huntington, K.W., 2014. Antecedence of the Yarlung–Siang–Brahmaputra River, eastern Himalaya. Earth Planet. Sci. Lett. 397, 145–158.
Lenard, S., 2019. The evolution of the Himalaya since the Late Miocene, as told by the history of its erosion. Earth Sciences. Université de Lorraine, 2019. English. NNT : 2019LORR0161.
Limonta, M., Garzanti, E., Resentini, A., 2023. Petrology of Bengal Fan turbidites (IODP Expeditions 353 and 354): provenance versus diagenetic control. J. Sediment. Res. 93 (4), 256–272.
Lupker, M., France-Lanord, C., Galy, V., Lavé, J., Gaillardet, J., Gajurel, A.P., Guilmette, C., Rahman, M., Singh, S.K., Sinha, R., 2012. Predominant floodplain over mountain weathering of Himalayan sediments (Ganga basin). Geochim. Cosmochim. Acta 84, 410–432.
Lupker, M., Lavé, J., France-Lanord, C., Christl, M., Bourlès, D., Carcaillet, J., Maden, C., Wieler, R., Rahman, M., Bezbaruah, D., Xiaohan, L., 2017. ^{10}Be systematics in the Tsangpo-Brahmaputra catchment: the cosmogenic nuclide legacy of the eastern Himalayan syntaxis. Earth Surf. Dyn. Disc. 2017, 1–29.
Malusà, M.G., Resentini, A., Garzanti, E., 2016. Hydraulic sorting and mineral fertility bias in detrital geochronology. Gondwana Res. 31, 1–19.
Matter, A., Ramseyer, K., 1985. Cathodoluminescence microscopy as a tool for provenance studies of sandstones. In: Zuffa, G.G. (Ed.), Provenance of Arenites. Springer Netherlands, Dordrecht, pp. 191–211.
Morin, G.P., Lavé, J., France-Lanord, C., Rigaudier, T., Gajurel, A.P., Sinha, R., 2018. Annual sediment transport dynamics in the Narayani basin, Central Nepal: assessing the impacts of erosion processes in the annual sediment budget. J. Geophys. Res. Earth 123, 2341–2376.
Müller, A., Knies, J., 2013. Trace elements and cathodoluminescence of detrital quartz in Arctic marine sediments–a new ice-rafted debris provenance proxy. Clim. Past 9 (6), 2615–2630.
Neuser, R.D., Richter, D.K., Vollbrecht, A., 1989. Natural quartz with brown-violet cathodoluminescence–genetic aspects evident from spectral analysis. Zbl Geol. Paläaont. Teil I 1988, 919–930.
Owen, M.R., Carozzi, A.V., 1986. Southern provenance of upper Jackfork Sandstone, southern Ouachita Mountains: cathodoluminescence petrology. Geol. Soc. Am. Bull. 97 (1), 110–115.
Padoan, M., Garzanti, E., Harlavan, Y., Villa, I.M., 2011. Tracing nile sediment sources by Sr and Nd isotope signatures (Uganda, Ethiopia, Sudan). Geochim. Cosmochim. Acta 75 (12), 3627–3644.
Pietsch, T.J., Olley, J.M., Nanson, G.C., 2008. Fluvial transport as a natural luminescence sensitiser of quartz. Quat. Geochronol. 3, 365–376.
Ramseyer, K., Mullis, J., 1990. Factors influencing short-lived blue cathodoluminescence of alpha-quartz. Am. Mineral. 75 (7–8), 791–800.
Ramseyer, K., Baumann, J., Matter, A., Mullis, J., 1988. Cathodoluminescence colours of α-quartz. Mineral. Mag. 52 (368), 669–677.
Ryb, U., Ponton, C., France-Lanord, C., Yoshida, K., Eiler, J.M., 2024. Late miocene uplift and exhumation of the lesser Himalaya recorded by clumped isotope compositions of detrital carbonate. Geophys. Res. Lett. 51 (21), e2024GL109643.
Sawakuchi, A.O., Blair, M.W., DeWitt, R., Faleiros, F.M., Hyppolito, T., Guedes, C.C.F., 2011. Thermal history versus sedimentary history: OSL sensitivity of quartz grains extracted from rocks and sediments. Quat. Geochronol. 6, 261–272.
Seyedolali, A., Krinsley, D.H., Boggs Jr., S., O'Hara, P.F., Dypvik, H., Goles, G.G., 1997. Provenance interpretation of quartz by scanning electron microscope–cathodoluminescence fabric analysis. Geology 25 (9), 787–790.
Sharp, Z.D., 1990. A laser-based microanalytical method for the in situ determination of oxygen isotope ratios of silicates and oxides. Geochim. Cosmochim. Acta 54 (5), 1353–1357.
Singh, S.K., France-Lanord, C., 2002. Tracing the distribution of erosion in the Brahmaputra watershed from isotopic compositions of stream sediments. Earth Planet. Sci. Lett. 202 (3–4), 645–662.
Spear, F.S., Pyle, J.M., 2002. Apatite, Monazite, and Xenotime in Metamorphic Rocks.
Sprunt, E.S., Dengler, L.A., Sloan, D., 1978. Effects of metamorphism on quartz cathodoluminescence. Geology 6 (5), 305–308.
Sridhar, K., Jackson, M.L., Clayton, R.N., 1975. Quartz oxygen isotopic stability in relation to isolation from sediments and diversity of source. Soil Sci. Soc. Am. J. 39 (6), 1209–1213.
Stalder, R., 2014. OH-defect content in detrital quartz grains as an archive for crystallisation conditions. Sediment. Geol. 307, 1–6.
Stalder, R., Konzett, J., 2012. OH defects in quartz in the system quartz–albite–water and granite–water between 5 and 25 kbar. Phys. Chem. Miner. 39, 817–827.
Stalder, R., Neuser, R.D., 2013. OH-defects in detrital quartz grains: potential for application as tool for provenance analysis and overview over crustal average. Sediment. Geol. 294, 118–126.

Stalder, R., Potrafke, A., Billström, K., Skogby, H., Meinhold, G., Gögele, C., Berberich, T., 2017. OH defects in quartz as monitor for igneous, metamorphic, and sedimentary processes. Am. Mineral. 102 (9), 1832–1842.
Stalder, R., Jaeger, D., Andò, S., Garzanti, E., Chiessi, C., Sawakuchi, A., Ludwig, T., Strasser, M., 2024. Trace element and OH content of quartz grains in the Amazon River: potential application in provenance studies. Sediment. Geol., SEDGEO10425 in review.
Suttner, L.J., Basu, A., Mack, G.H., 1981. Climate and the origin of quartz arenites. J. Sediment. Res. 51 (4), 1235–1246.
Syers, J.K., Jackson, M.L., Berkheiser, V.E., Clayton, R.N., Rex, R.W., 1969. Eolian sediment influence on pedogenesis during the Quaternary. Soil Sci. 107 (6), 421–427.
Szulc, A.G., Najman, Y., Sinclair, H.D., Pringle, M., Bickle, M., Chapman, H., Garzanti, E., Andò, S., Huyghe, P., Mugnier, J.-L., Ojha, T., DeCelles, P., 2006. Tectonic evolution of the Himalaya constrained by detrital 40Ar–39Ar, Sm–Nd and petrographic data from the Siwalik foreland basin succession, SW Nepal. Basin Res. 18 (4), 375–391.
Taylor, H.P., 1968. The oxygen isotope geochemistry of igneous rocks. Contrib. Mineral. Petrol. 19, 1–71.
Taylor Jr., H.P., Coleman, R.G., 1968. O^{18}/O^{16} ratios of coexisting minerals in glaucophane-bearing metamorphic rocks. Geol. Soc. Am. Bull. 79 (12), 1727–1756.
Taylor Jr., H.P., Epstein, S., 1962. Oxygen isotope studies on the origin of tektites. J. Geophys. Res. 67 (11), 4485–4490.
Taylor Jr., H.P., Sheppard, S.M.F., 1986. Igneous rocks; I, Processes of isotopic fractionation and isotope systematics. Rev. Mineral. Geochem. 16 (1), 227–271.
Timar-Gabor, A., Kabacińska, Z., Constantin, D., Dave, A.K., Buylaert, J-P., 2023. Reconstructing dust provenance from quartz optically stimulated luminescence (OSL) and electron spin resonance (ESR) signals: preliminary results on loess from around the world. Radiat. Phys. Chem. 212, 111138. https://doi.org/10.1016/j.radphyschem.2023.111138.
Valley, J.W., Kita, N.T., Fayek, M., 2009. In situ oxygen isotope geochemistry by ion microprobe. MAC Short Course 41, 19–63.
Vennemann, T.W., Kesler, S.E., O'Neil, J.R., 1992. Stable isotope compositions of quartz pebbles and their fluid inclusions as tracers of sediment provenance: Implications for gold-and uranium-bearing quartz pebble conglomerates. Geology 20 (9), 837–840.
Vennemann, T.W., Kesler, S.E., Frederickson, G.C., Minter, W.E.L., Heine, R.R., 1996. Oxygen isotope sedimentology of gold-and uranium-bearing Witwatersrand and Huronian Supergroup quartz-pebble conglomerates. Econ. Geol. 91 (2), 322–342.
Walderhaug, O., Rykkje, J., 2000. Some examples of the effect of crystallographic orientation on the cathodoluminescence colors of quartz. J. Sediment. Res. 70 (3), 545–548.
Weil, J.A., 1984. A review of electron spin spectroscopy and its application to the study of paramagnetic defects in crystalline quartz. Phys. Chem. Miner. 10 (4), 149–165.
Williams, O.M., Spooner, N.A., Smith, B.W., Moffatt, J.E., 2018. Extended duration optically stimulated luminescence in quartz. Radiat. Meas. 119, 42–51. https://doi.org/10.1016/j.radmeas.2018.09.005.
Williams, O.M., Smith, B.W., Spooner, N.A., 2022. A role for oxygen vacancies in quartz luminescence. Radiat. Meas. 154, 106774.
Zhang, A., Gao, Q., Rahman, S.M., Alam, M.M., Guo, Y., Chen, Y., Cheng, J., Wang, H., Wang, P., Zhang, J., Yi, C., Hu, G., 2023. Luminescence fingerprints fluvial sediment transport from the Tibetan Plateau to the Bangladesh Delta. Earth Planet. Sci. Lett. 622, 118387.
Zinkernagel, U., 1978. Cathodolumnescence of quartz and its applications to sandstone petrology. Contrib. Sedimentol. 8, 1–69.